EUROPEAN FUSION DEVELOPMENT AGREEMENT

EFDA–JET–CP(01)02-17

W.Suttrop, R.Budny, J.G.Cordey, C.Gowers, M.Mantsinen, G.Matthews, H.Nordman, V.Parail, JRapp, J.Storrs, J.Strachan, J.Weiland, K.D.Zastrow and JET EFDA Contributors

Effect of Heat Flux and Density Variation on Electron Temperature Profiles in JET ELMy H-modes

Effect of Heat Flux and Density Variation on Electron Temperature Profiles in JET ELMy H-modes

W.Suttrop[1], R.Budny[2], J.G.Cordey[3], C.Gowers[3], M.Mantsinen[4], G.Matthews[3], H.Nordman[5], V.Parail[3], JRapp[6], J.Storrs[3], J.Strachan[2], J.Weiland[5], K.D.Zastrow[3] and JET EFDA Contributors*

[1]Max-Planck-Institut für Plasmaphysik, EURATOM Association, Garching, Germany
[2]Princeton Plasma Physics Laboratory, Princeton, N.J., U.S.A.
[3]UKAEA Fusion, Culham Laboratory, Euratom Association, Abingdon, U.K.
[4]Association EURATOM-Tekes, Helsinki University of Technology, Finland
[5]Chalmers Technical University, Gothenburg, Sweden
[6]Forschungszentrum Jülich, EURATOM Association, Jülich, Germany
** See the appendix of JET EFDA contributors (prepared by J. Paméla and E.R Solano),*
**See appendix of the paper by J.Pamela "Overview of recent JET results",*
Proceedings of the IAEA conference on Fusion Energy, Sorrento 2000

Preprint of Paper to be submitted for publication in Proceedings of the
EPS Conference,
(Maderia, Portugal 18-22 June 2001)

ABSTRACT

A class of transport-relevant instabilities, including Ion Temperature Gradient (ITG), Trapped Electron (TEM) and Electron Temperature Gradient (ETG) driven modes induce a heat flux which increases strongly with temperature gradient above a certain threshold of the inverse temperature gradient length $1/L_T \equiv T'/T$. This behaviour can be recognised experimentally in various ways: 1. At sufficiently high heat flux the ion and electron temperature gradient length is clamped at a critical value ("stiffness" of profiles), 2. the "incremental" heat transport coefficient $\chi_{inc} \equiv (1/n) \partial q_\perp / \partial \nabla T$ is larger than the heat flux coefficient derived from local power balance $\chi_{pb} \equiv (1/n) q_\perp / \nabla T$ and 3. Edge and core temperatures are proportional and for typically flat H-mode density profiles a strong relation between edge pedestal pressure and total stored energy is found. Evidence for critical gradients from all three methods has been found experimentally, e.g. in ASDEX Upgrade for ion [1, 2] and electron [3] transport channels. In JET, previous experiments with on- and off-axis deposited ICRH [4] resulted in weak variation of the transport coefficients with heat flux. The current investigation aims to extend these studies in JET by application of increased ICRH power and variation of the edge temperature at each heating power level.

1. EXPERIMENT

The experiments reported here are carried out in JET plasmas with low triangularity ($\delta \approx 0.3$) and boundary shape suited for optimum coupling of ICRH power. Deuterium plasmas with a hydrogen content of about 3-5% are used for first harmonic ICRH minority heating. Part of the heating power is absorbed by the main ions in second harmonic. RF frequencies are 42MHz for central deposition and 37MHz for off-axis deposition at a toroidal field of $B_t = 2.8$T. The plasma current used is $I_p = 2.8$MA. The coupled ICRH power is varied between 6 and 10.5MW. The NBI power is chosen for fixed total heating power of 14MW in all cases. The electron density is varied by external deuterium gas puffing and ranges from 2.5×10^{19} m^{-3} to 6×10^{19} m^{-3}, corresponding to 25-60% of the Greenwald density limit.

Figure 1 shows time traces for a typical pulse. Combined ICRH and NBI heating are applied immediately after the plasma current has been ramped up. Early transition to H-mode and consequently high plasma temperature leads to delayed current diffusion before the central safety factor q_0 reaches unity. This technique provides a sawtooth-free H-mode phase of about 3 seconds or 10 confinement times. Subsequently all measurements are taken during this time interval in order to study transport without interference of sawtooth effects on core profiles. Figure 2 shows the radial heat flux calculated with the PION code [5] for three selected pulses with 6MW ICRH power and on-axis and off-axis reonance and 10MW on-axis ICRH power. The fast particle populations (H and D) are calculated taking into account combined ICRH and NBI heating. With increasing ICRH power more collisional electron heating is obtained as ICRH tends to create energetic ions that slow down in collisions mainly with electrons. As a result, the electron heat flux varies strongly, from 6 to 55kW/m^2 at $\rho = 0.4$, with ICRH power applied. At the moderate densities

and high temperatures encountered in the experiment (central T_e up to 8keV), ions and eletrons are only weakly coupled and the ion heat flux does not show strong variations.

TEMPERATURE PROFILE RESPONSE

The electron and ion temperatures measured during the sawtooth-free phases of the plasmas of Fig. 2 are plotted in Fig. 3 on a linear (Fig. 3a) and a logarithmic scale (Fig. 3b). These representations have been chosen to demonstrate variations of temperature gradients and gradient lengths, respectively. A significant change of electron temperature gradient is found when changing from 6MW off-axis to on-axis ICRH deposition, in agreement with previous measurements at JET [4]. For further increased electron heat flux (centrally deposited ICRH power up to 10.5MW), the temperature gradient and gradient length are changing only weakly. As can be seen from Fig. 2, the electron heat flux varies most strongly near mid-radius.

DISCUSSION

For on-axis heating, most of the ICRH power is absorbed near the plasma centre and plasma heating by slowing-down of fast ions is mainly inside the inner half of the plasma radius. As measurements are taken during sawtooth-free phases, broadening due to re-distribution of fast particles during sawtooth crashes does not have to be considered. The neutral beam power deposition profile is broad and a large fraction of beam power is deposited outside mid-radius. Thus, variation of the ratio of ICRH and NBI power leads to strong variation of the heat flux near mid-radius (Fig. 2). We can plot the perpendicular heat flux carried by electrons ($q_{e,\perp}$) at a normalized poloidal flux radius $r_p = 0.4$ as a function of inverse electron temperature gradient length $1/L_T = \nabla T_e / T_e$ (Fig. 4). At high heat flux ($q_{e,\perp} > 0.03 MW/m^2$), $\nabla T_e / T_e$ depends only weakly on electron heat flux, indicating a saturation near $\nabla T_e / T_e \approx 3m^{-1}$, corresponding to $R / L_{T_e} = 9$(for major radius R = 3m). For low heat flux ($q_{e,\perp} \leq 0.03 MW/m^2$), the profile variation seen in Ref. [4] at the same level of heating power is reproduced. On- and off-axis deposition at $P_{ICRH} = 6MW$ results in a significant different gradient length. These results indicate that in JET critical electron temperature gradients are reached only for highest heat flux, which can be obtained only for high centrally deposited ICRH power.

It is interesting to compare the JET results with observations on other tokamaks where gradient length saturation is seen. For ohmic and ECRH heated plasmas at low density in ASDEX Upgrade [3] nearly unchanged gradient lengths are found for a wide range of heat fluxes $q_{e,\perp} = 0.012...0.1 MW/m2$. R / L_{T_e} is found radius-dependent. In Tore Supra plasmas with Fast Wave (FW) heating [6], also a radius-dependent critical electron temperature gradient is found. The radial dependence in both experiments can be accounted for if the electron heat flux is normalised by a factor of $T^{3/2}$, consistent with a gyro-Bohm scaling of radial transport coefficients. For the present JET experiments, saturation of $\nabla T_e / T_e$ sets in around $q_{e,\perp} = 0.03 MW/m^2$, which is similar or higher than that reported in Refs. [3] and [6], but $q_e/T_e^{3/2}$ (Fig. 5) is about an order of magnitude lower. A gyro-Bohm scaling of the heat flux ($q_\perp \propto T^{3/2}$) is also consistent with the present JET data (Fig. 5).

Predictive JETTO simulations are made to compare experimental core temperature profiles with the ITG/TEM based Weiland model [7] and the semi-empirical mixed Bohm/gyro-Bohm model [8] for JET plasmas. With density profiles and edge temperature (at 90% flux) taken from the experiment core T_i and T_e profiles are predicted typically with an accuracy of 30% or better. A profile comparison for on- and off-axis heated plasmas (P_{ICRH} = 6MW) is shown in Fig. 6. For this particular case with low central heat flux, where L_{T_i} and L_{T_e} show some variation, the first-principle based Weiland model tends to slightly over-estimate the stiffness of T_i. The model can also account for the observed electron transport, but further study is needed to quantify the relative contribution of trapped electron modes (included) and electron temperature gradient-driven modes (not included in the model).

REFERENCES

[1]. W. Suttrop, et al., Plasma Phys. Controlled Fusion 39 (1997) 2051.

[2]. J. Stober, et al., Plasma Phys. Controlled Fusion 42 (2000) A211.

[3]. F. Ryter, et al., Phys. Rev. Lett. 86 (2001) 2325.

[4]. J.P. Christiansen, et al., in Proc. of the 26th EPS Conference on Controlled Fusion and Plasma Physics, Maastricht, 1999, pages 209–212, Geneva, 1999, EPS.

[5]. L.-G. Eriksson, T.Hellsten, and U.Will´en, Nucl. Fusion 33 (1993) 1037.

[6]. G.T. Hoang, et al., IAEA conference on Plasma Physics and Controlled Nuclear Fusion Research, Sorrento, 2000; proceedings to be published

[7]. H. Nordman, J.Weiland, and A.Jarmen, Nucl. Fusion 30 (1990) 983.

[8]. M. Erba, et al., Plasma Phys. Controlled Fusion 39 (1997) 261.

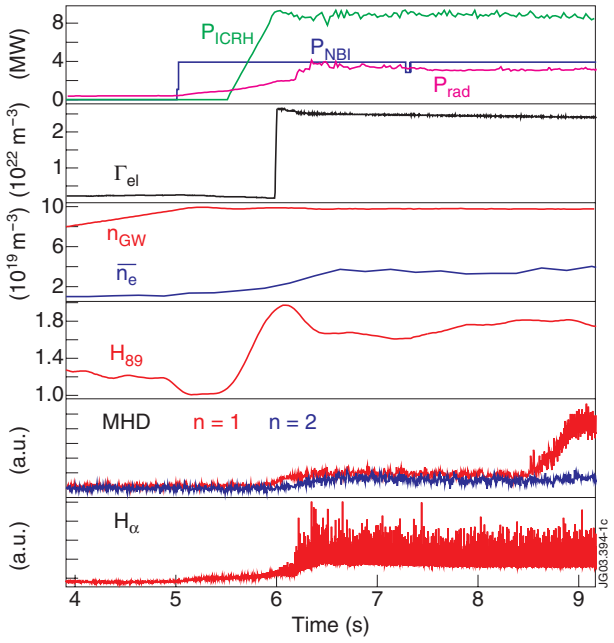

Figure 1: Time traces of transport experiments. Data is taken around t = 7s during a sawtooth-free type III ELMy H-mode phase.

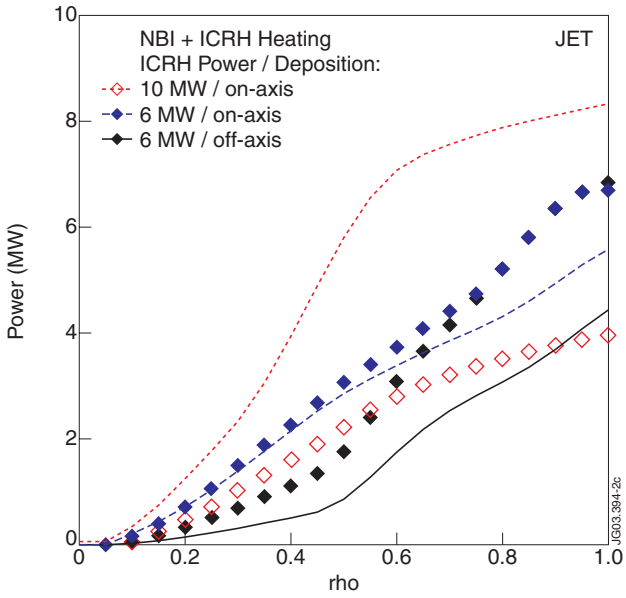

Figure 2: Total radial heat flux carried by electron (solid lines) and ions (symbols) for on- and off-axis ICRH heating (ICRH power 6 and 10MW). Total injected power (ICRH+NBI) is 14MW.

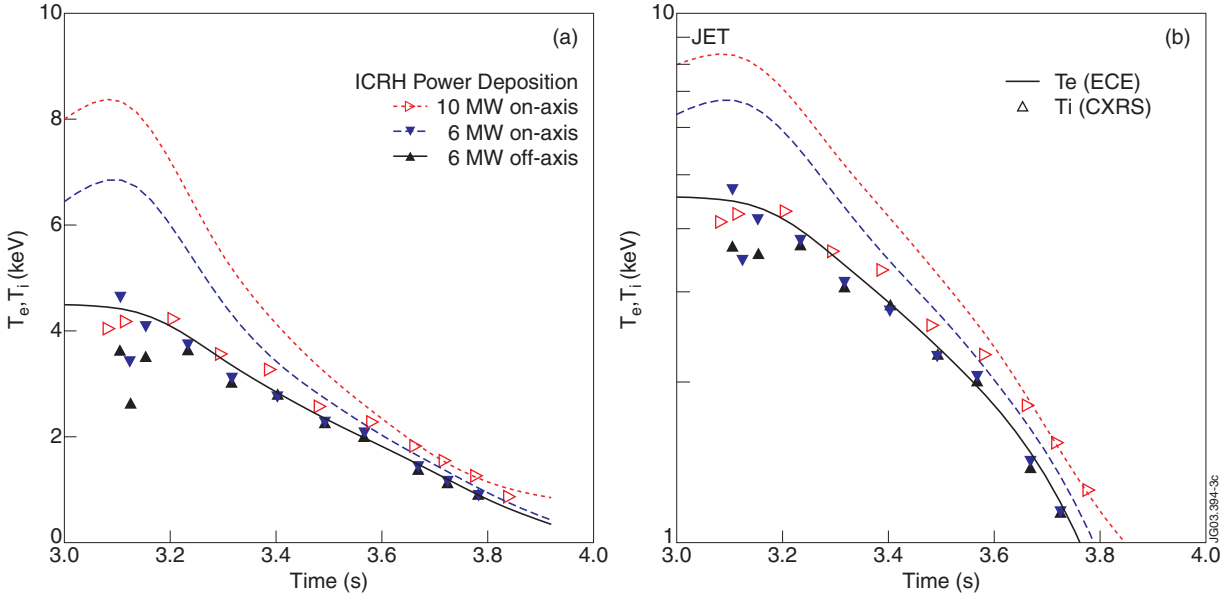

Figure 3: Electron and ion temperature profiles for different ICRH power and deposition radius (see Fig. 2): (a) linear, (b) logarithmic scale.

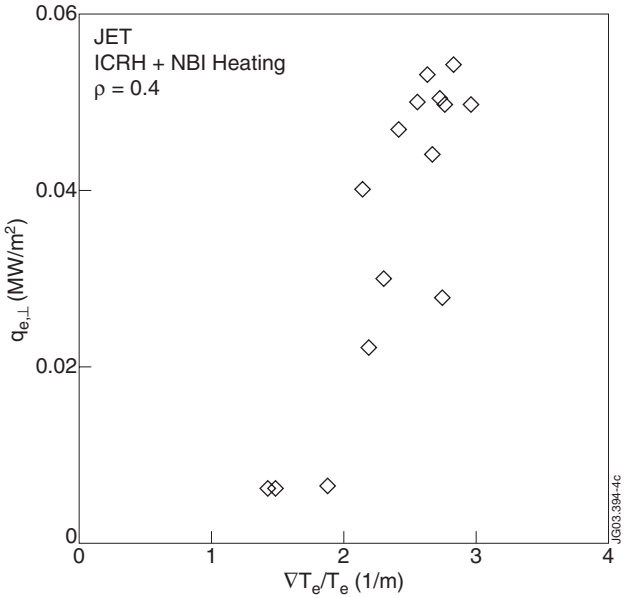

Figure 4: Electron heat flux at ρ_p = 0.4 as a function of inverse electron temperature gradient length.

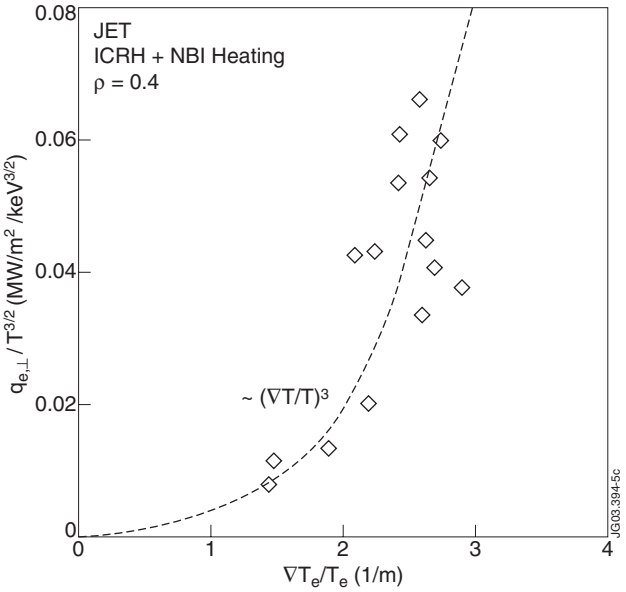

Figure 5: As before, but heat flux normalized to $T_e^{3/2}$. A functional dependence $\propto (\nabla T = T)^3$ is indicated for comparison.

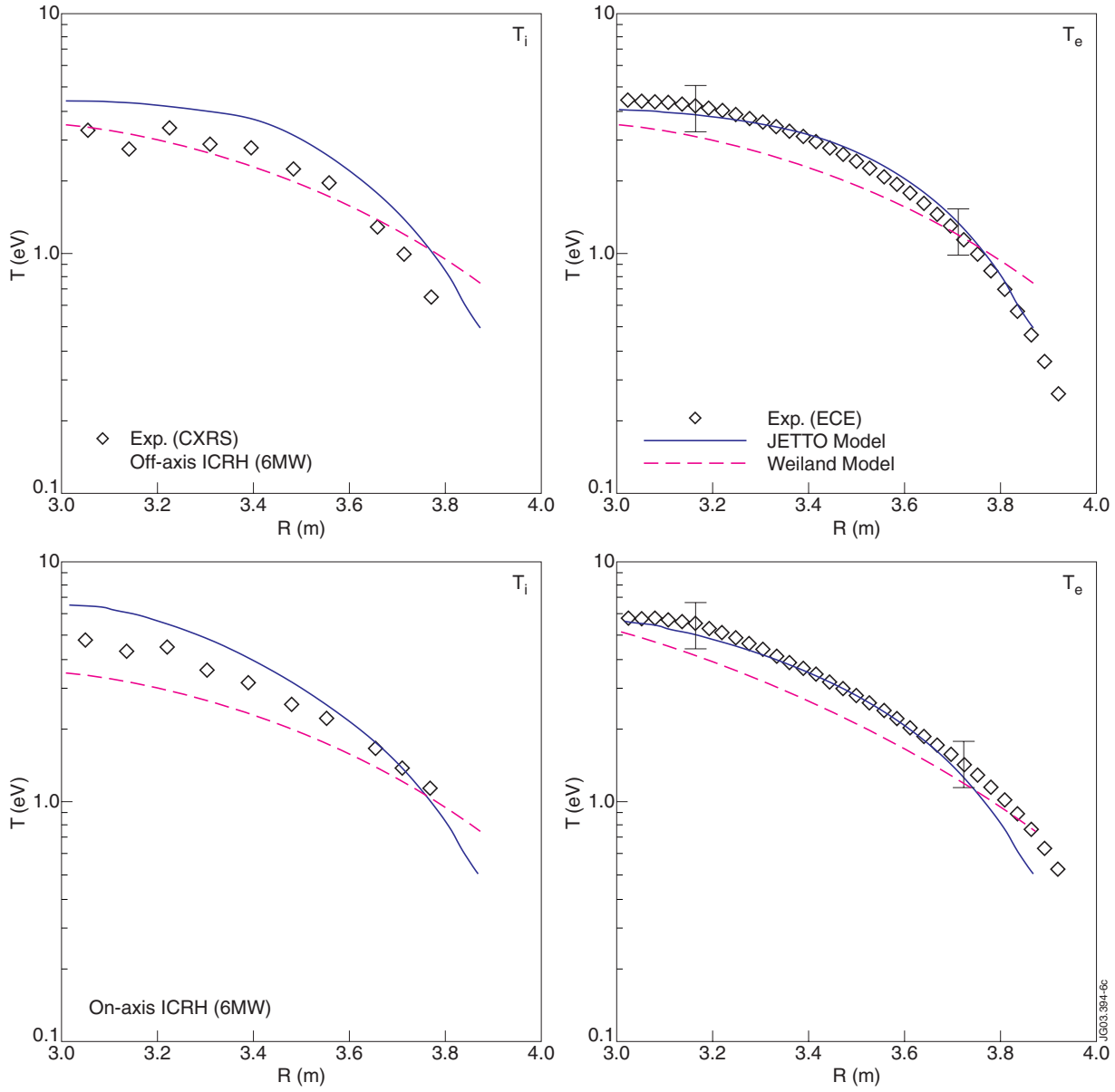

Figure 6: Comparison of T_i (left) and T_e (right) profiles with transport models (see text) for off-axis (top) and on-axis (bottom) ICRH heating.